

# K<sup>-</sup> Meson Production in the Proton–Proton Reaction at 3.67 GeV/c

F. Balestra<sup>d</sup> Y. Bedfer<sup>c</sup> R. Bertini<sup>c,d</sup> L.C. Bland<sup>b</sup>  
 A. Brenschede<sup>h,1</sup> F. Brochard<sup>c,2</sup> M.P. Bussa<sup>d</sup>  
 V. Tchalyshev<sup>a</sup> Seonho Choi<sup>b,3</sup> M. Debowski<sup>f,4</sup>  
 M. Dzemidzic<sup>b,5</sup> J.-Cl. Faivre<sup>c</sup> I.V. Falomkin<sup>a</sup> L. Fava<sup>e</sup>  
 L. Ferrero<sup>d</sup> J. Foryciarz<sup>g,f,6</sup> I. Fröhlich<sup>h</sup> V. Frolov<sup>a</sup>  
 R. Garfagnini<sup>d</sup> D. Gill<sup>j</sup> A. Grasso<sup>d</sup> E. Grosse<sup>i</sup> S. Heinz<sup>c</sup>  
 V.V. Ivanov<sup>a</sup> W.W. Jacobs<sup>b</sup> W. Kühn<sup>h</sup> A. Maggiora<sup>d</sup>  
 M. Maggiora<sup>d</sup> A. Manara<sup>c,d</sup> D. Panzieri<sup>e</sup> H.-W. Pfaff<sup>h</sup>  
 G. Piragino<sup>d</sup> G.B. Pontecorvo<sup>a</sup> A. Popov<sup>a</sup> J. Ritman<sup>h</sup>  
 P. Salabura<sup>f</sup> F. Tosello<sup>d</sup> S.E. Vigdor<sup>b</sup> G. Zosi<sup>d</sup>

<sup>a</sup>*JINR, Dubna, Russia*

<sup>b</sup>*Indiana University Cyclotron Facility, Bloomington, Indiana, U.S.A.*

<sup>c</sup>*Laboratoire National Saturne, CEA Saclay, France*

<sup>d</sup>*Dipartimento di Fisica “A. Avogadro” and INFN - Torino, Italy*

<sup>e</sup>*Universita’ del Piemonte Orientale and INFN - Torino, Italy*

<sup>f</sup>*M. Smoluchowski Institute of Physics, Jagellonian University, Kraków, Poland*

<sup>g</sup>*H.Niewodniczanski Institute of Nuclear Physics, Kraków, Poland*

<sup>h</sup>*II. Physikalisches Institut, University of Gießen, Germany*

<sup>i</sup>*Forschungszentrum Rossendorf, Dresden, Germany*

<sup>j</sup>*TRIUMF - Vancouver, Canada*

DISTO Collaboration

---

## Abstract

The total cross section of the reaction  $pp \rightarrow ppK^+K^-$  has been determined for proton–proton reactions with  $p_{beam} = 3.67 \text{ GeV}/c$ . This represents the first cross section measurement of the  $pp \rightarrow ppK^-K^+$  channel near threshold, and is equivalent to the inclusive  $pp \rightarrow ppK^-X$  cross section at this beam momentum. The cross section determined at this beam momentum is about a factor 20 lower than that for inclusive  $pp \rightarrow ppK^+X$  meson production at the same CM energy above the corresponding threshold. This large difference in the  $K^+$  and  $K^-$  meson

inclusive production cross sections in proton-proton reactions is in strong contrast to cross sections measured in sub-threshold heavy ion collisions, which are similar in magnitude at the same energy per nucleon below the respective thresholds.

*Key words:* antikaon, near-threshold meson production

*PACS:* 25.40.Ve, 13.75.Cs, 13.85.Hd, 13.85.Ni

---

## 1 INTRODUCTION

Currently there is much interest to determine the total  $K^-$  meson production cross section in nucleon-nucleon reactions near threshold. This cross section is of particular importance in heavy-ion physics. In heavy ion collisions it has been observed that the inclusive production cross sections for  $K^-$  and  $K^+$  mesons are nearly equal in sub-threshold reactions when measured at the same energy per nucleon below the production thresholds for the reactions  $pp \rightarrow K^-X$  and  $pp \rightarrow K^+X$ , respectively [1]. This result is surprising for several reasons. First, the  $K^-$  production cross section in near-threshold proton-proton reactions is expected [2] to be lower by over an order of magnitude than the  $K^+$  cross section at the same distance from their respective thresholds. Second, antikaons ( $K^-, \bar{K}^0$ ) should have a higher absorption probability in heavy ion collisions than kaons ( $K^+, K^0$ ), primarily as a result of strangeness exchange reactions (e.g.  $K^-N \rightarrow Y\pi$  with  $Y = \Lambda, \Sigma$ ). Although charge exchange reactions (e.g.  $K^+n \rightarrow K^0p$ ) may occur, changes to the observed yield of a particular charge state will be largely compensated by the corresponding reverse process. In this context it has been shown in detailed model calculations that multi-step processes can not explain the enhanced  $K^-$  yield in heavy ion reactions [3]. A promising explanation of this discrepancy comes from various theoretical models [4] which suggest that, as a result of partial chiral symmetry restoration in a dense hadronic medium, antikaons are subject to strongly attractive, and kaons to slightly repulsive, forces. These effective interactions would lower the apparent  $K^-$  production threshold in a dense hadronic medium, and thus enhance the  $K^-$  yield in heavy ion collisions.

However, the comparison of heavy ion with nucleon-nucleon collisions has relied on some assumptions because, in the latter case, the antikaon data

---

<sup>1</sup> current address: Brokat Infosystems AG - Stuttgart

<sup>2</sup> current address: LPNHE X, Ecole Polytechnique Palaiseau

<sup>3</sup> current address: Temple University, Philadelphia

<sup>4</sup> current address: FZ-Rosendorf

<sup>5</sup> current address: IU School of Medicine - Indianapolis

<sup>6</sup> current address: Motorola Polska Software Center - Krakow

were either deduced from  $pp \rightarrow ppK_0\bar{K}_0$  results, or taken as the sum of different exclusive channels with one or two pions in the final state [2]. Furthermore, apart from a preliminary upper limit [5], there is a lack of pp antikaon production data in the regime of available energy most relevant in near-threshold heavy ion collisions (i.e.  $\sqrt{s} - \sqrt{s_0} < 0.5 \text{ GeV}$ , where  $\sqrt{s_0}$  is the threshold of the particular channel under consideration) [6]. The result presented in this work represents the first cross section determination of the exclusive channel  $pp \rightarrow ppK^+K^-$ , and is equivalent to the inclusive  $K^-$  production cross section since no other purely hadronic channels including  $K^-$  are kinematically allowed at the beam momentum of this experiment (i.e.  $\sqrt{s} - \sqrt{s_0} = 111 \text{ MeV} < M_{\pi^0}c^2$ ).

## 2 EXPERIMENTAL PROCEDURE

### 2.1 Apparatus

A proton beam from the SATURNE proton synchrotron with momentum  $p_{beam} = 3.67 \text{ GeV}/c$  was directed onto a liquid hydrogen target of 2 cm length. All events with at least four charged particles in the final state were measured with the DISTO spectrometer, which is described in detail elsewhere [7]. Charged particles were tracked through a magnetic spectrometer which consisted of a dipole magnet ( $\sim 1.0 \text{ T} \cdot \text{m}$ ), two sets of scintillating fiber hodoscopes inside the field and 2 sets of multi-wire proportional chambers (MWPC) outside the field. Furthermore, two arrays of scintillator hodoscopes and water Čerenkov detectors were located behind the MWPCs. Particle identification was performed using the correlation between the particle momenta and the Čerenkov light output (see also [7]). The large acceptance of the spectrometer ( $\approx \pm 15^\circ$  vertical,  $\approx \pm 48^\circ$  horizontal in the laboratory reference frame) guarantees a sizeable efficiency for coincident detection of four charged particles. The measurement of all particles in the final state allowed 4-momentum conservation to be used in addition to particle identification for effective background suppression in order to identify the  $ppK^+K^-$  final state.

### 2.2 Data Selection

Since the 4-momenta of all particles in the final state were measured, the events are kinematically over-determined. Therefore, 4-momentum conservation can be used for a substantial background suppression by requiring that the proton-proton missing mass ( $M_{miss}^{pp}$ ) be equal to the  $K^+K^-$  invariant mass ( $M_{inv}^{KK}$ ). The distribution of  $(M_{inv}^{KK})^2 - (M_{miss}^{pp})^2$  is plotted in Figure 1. The

peak near  $(M_{inv}^{KK})^2 - (M_{miss}^{pp})^2 = 0$  results from events where the  $ppK^+K^-$  event hypothesis was correct, and is the basis for the cross section values quoted below. This peak is superimposed on a background resulting from imperfect  $\pi - K$  separation in the Čerenkov detectors in a small fraction of events of the type  $pp \rightarrow pK^+\Lambda \rightarrow ppK^+\pi^-$  or  $pp \rightarrow pp\pi^+\pi^-X$ . An estimate of the background underneath the  $ppK^+K^-$  peak is given by the solid curve in Fig. 1. This estimate was determined by scaling the  $(M_{inv}^{KK})^2 - (M_{miss}^{pp})^2$  distribution, measured for all events before requiring kaon identification, by a factor 0.002 in order to match the data in Fig. 1 above  $0.15 \text{ GeV}^2/c^4$ . From this histogram it is determined that the background accounts for about 13% of the yield in Fig. 1 with  $|(M_{inv}^{KK})^2 - (M_{miss}^{pp})^2| < 0.09 \text{ GeV}^2/c^4$ . This background has been subtracted in the subsequent analysis as described below. To extract a total cross section from the data shown in Fig. 1, a correction for the detector acceptance and an absolute normalization must also be determined.

### 2.3 Acceptance Corrections

The correction of the measured yields for the detector acceptance has been evaluated by means of Monte Carlo simulations, which after digitization of the simulated detector hits, were processed through the same analysis chain as the measured data. The detector acceptance was determined as a multi-dimensional function of the relevant kinematic degrees of freedom of the particles in the final state. After accounting for the azimuthal and reflection symmetries, the detector acceptance was non-zero over the full kinematically allowed region. Thus, the acceptance correction is essentially independent of the actual phase space distribution of the final state, and has been determined assuming a uniform phase space distribution in the simulations. This has been verified by calculating the acceptance correction matrix using different initial distributions in the simulations, and observing that the measured yield varied less than the systematic error associated to the acceptance correction. Although eight linearly independent degrees of freedom are in principle required to fully describe the  $pp \rightarrow ppX \rightarrow ppK^+K^-$  reaction, a five dimensional acceptance correction matrix is sufficient, in part because the cross section cannot depend upon the azimuthal orientation of the event. Furthermore, we have compared the observed angular distribution of the  $X \rightarrow K^+K^-$  decay with that from simulations. The comparison of data with simulations has a  $\chi^2/n = 1.4$  for a S-wave distribution and a  $\chi^2/n = 17.6$  for a P-wave distribution. Therefore, in the simulations uniform distributions with respect to these three angular variables were integrated over when determining the acceptance as a function of the remaining five variables. Finally, the raw data were corrected on an event-by-event basis, via a weighting factor determined from the simulated acceptance function for the appropriate kinematic bin.

Since the acceptance varies as a function of the kinematic distribution of the final state, one can not simply reduce the acceptance to a single number without making assumptions about the phase space distribution of the particles in the final state. Nevertheless, a reasonable estimate of the average acceptance can be determined for kaon pairs with an invariant mass equal to the phi meson mass (where most of the measured kaon pairs are observed) and an isotropic distribution in the other kinematic variables. In this case the product of the geometrical acceptance times the tracking reconstruction efficiency is 21.4%.

#### 2.4 Background Subtraction

The background contribution from non- $ppK^+K^-$  events, shown as the solid curve in Fig. 1, must be subtracted from the data in order to determine the  $K^+K^-$  yield. The subtraction was performed on the  $M_{inv}^{KK}$  distribution. For this, the  $M_{inv}^{KK}$  distribution for the background events was determined by applying the acceptance correction matrix (determined for simulated  $pp \rightarrow ppK^+K^-$  reactions) to events subjected to the same kinematic requirement  $|(M_{inv}^{KK})^2 - (M_{miss}^{pp})^2| < 0.09 \text{ GeV}^2/c^4$ , but not to the kaon identification conditions with the Čerenkov detectors. The resulting distribution was scaled by the same factor (0.002) used by the solid curve in Fig. 1, and then subtracted from the acceptance corrected  $M_{inv}^{KK}$  distribution that included both  $ppK^+K^-$  and background events. Finally, the  $M_{inv}^{KK}$  spectrum, after full acceptance corrections and background subtraction, is shown in Figure 2. The curves are fits to the data as described below.

#### 2.5 Absolute Normalization

The absolute normalization of the  $ppK^+K^-$  cross section was determined by measuring the yield relative to that of a *simultaneously* measured channel with known cross section. For this work the reference channel was the reaction  $pp \rightarrow pp\eta$  for which a large amount of data exist [8]. This method to determine the absolute normalization was chosen because it greatly reduced the large systematic uncertainty associated with the absolute calibrations of both beam intensity and absolute trigger efficiency. In order to provide the absolute cross section calibration the existing published data was first interpolated to get the  $\eta$  production cross-section at the beam momentum of the present measurement, and then the appropriate acceptance corrections were applied to determine the  $K^+K^-/\eta$  total cross section ratio from our yields.

The cross section of the reaction  $pp \rightarrow pp\eta$  has been interpolated to our beam momentum with several parameterizations that vary smoothly with beam mo-

mentum. From these interpolations we estimate the exclusive  $pp \rightarrow pp\eta$  production cross section to be  $135 \pm 35 \mu b$  at  $p_{beam} = 3.67 \text{ GeV}/c$ . The parameterizations describe the existing  $\eta$  production data well with the exception of the single measurement at  $p_{beam} = 2.8 \text{ GeV}/c$  by E. Pickup et al. [9] which is significantly underestimated. This discrepancy has been neglected since that measurement is subject to a large systematic error associated with a quite substantial background subtraction.

In the present data, the  $\eta$  meson has been identified in the  $M_{miss}^{pp}$  distribution for  $pp\pi^+\pi^-X$  events, after requiring that the four particle missing mass be consistent with  $M_{\pi^0}$  as shown in Ref. [13]. The acceptance correction of the  $pp \rightarrow pp\eta \rightarrow pp\pi^+\pi^-\pi^0$  channel was performed similarly to the  $pp \rightarrow ppK^+K^-$  discussed above. The acceptance correction matrix for the  $pp\eta$  channel has four dimensions. These are sufficient to completely describe this 5 body final state because the full set of 15 kinematic degrees of freedom (dof) is reduced by four-momentum conservation (-4 dof), the azimuthal symmetry of the event (-1 dof), the requirement that  $M_{miss}^{pp} = M_{\eta}$  (-1 dof), the isotropic orientation of the  $\eta$  meson decay plane (-3 dof), and the known matrix element (-2 dof) for the  $\eta \rightarrow \pi^+\pi^-\pi^0$  decay [10].

### 3 Results

#### 3.1 Total $K^+K^-$ Cross Section

After applying the full acceptance corrections to the  $pp \rightarrow ppK^+K^-$  and  $pp \rightarrow pp\eta \rightarrow pp\pi^+\pi^-\pi^0$  channels, the  $K^+K^-/\eta$  total cross section ratio is determined to be  $(1.5 \pm 0.1(stat.) \pm 0.4(sys.)) \times 10^{-3}$ . The systematic error quoted here arises from the quadratic sum of the uncertainties on the  $\eta$  and  $K^+K^-$  background subtractions (15% and 5% respectively), relative acceptance correction (11%), trigger bias (10%), tracking efficiency (10%), and the Čerenkov particle identification efficiency (14%). This value has also been corrected for systematic bias effects due to the different scintillating fiber efficiencies for pions and kaons (-7.5%) and from the subtraction of events arising from the target envelope (+5%). Based on the  $\eta$  cross section estimated above in Sec. 2.5, a total cross section for the reaction  $pp \rightarrow ppK^+K^-$  of  $(0.20 \pm 0.011 \pm 0.08)\mu b$  has been determined, where the second error quoted here is the quadratic sum of the systematic uncertainty in the measured yield ratio and the absolute normalization uncertainty for the  $\eta$  production cross section.

The present total  $pp \rightarrow ppK^+K^-$  cross section value is plotted as the solid data point in Figure 3, where it is compared with estimates of  $K^-$  inclusive produc-

tion cross sections at higher energy (open circles) taken from the literature [2]. These additional data points have been deduced from other reactions either by assuming  $\sigma_{pp \rightarrow K^- X} = \sigma_{pp \rightarrow \bar{K}^0 X}$ , or by taking the sum of exclusive channels with one or two pions in the final state. The solid curve, corresponding to a prediction from Sibirtsev et al. [11] using a one meson exchange model including  $\pi$ ,  $K$ , and  $K^*$  mesons, accounts well for the  $K^-$  cross section measured in this experiment near the production threshold. In comparison, the total cross sections for inclusive  $K^+$  production shown as the open diamonds [12] in Fig. 3, are more than an order of magnitude larger at comparable distances above the  $K^+$  threshold.

### 3.2 $\phi$ Meson

Near threshold the  $K^-$  meson is produced, to a large degree, by the decay of the  $\phi$  meson as an intermediate state [13]. The fraction of the cross section from the resonant production can be determined from the  $M_{inv}^{KK}$  distribution. The  $M_{inv}^{KK}$  spectrum in Fig. 2 has been fit with the sum of a non-resonant contribution and a peak from the  $\phi$  resonance. The shape of the non-resonant contribution was assumed to be given by the  $M_{inv}^{KK}$  distribution for an ensemble of events that are uniformly distributed according to four body ( $ppK^+K^-$ ) phase space. The shape of the  $\phi$  resonance was given by the natural line-shape folded with a Gauss function to account for the detector resolution. When treating the width ( $\sigma$ ) of the Gaussian as a free parameter, we find an optimal fit with  $\sigma = 3.5 \pm 0.5 \text{ MeV}/c^2$ , in good agreement with simulations of the detector performance.

The total  $K^+K^-$  cross section value, as well as the resonant and non-resonant components, are summarized in Table 1. After correction for the corresponding partial width [14], the total  $\phi$  meson production cross section is  $0.19 \pm 0.014 \pm 0.08 \mu b$ . The systematic errors quoted have the same meaning as explained above.

Table 1

Total exclusive production cross section for the reaction  $pp \rightarrow ppK^+K^-$  at 3.67 GeV/c and for the resonant ( $\phi$  meson) and non-resonant contributions.

Meson Species	Cross Section [ $\mu b$ ]
total $K^+K^-$	$0.20 \pm 0.011 \pm 0.08$
$\phi \rightarrow K^+K^-$	$0.09 \pm 0.007 \pm 0.04$
non-resonant $K^+K^-$	$0.11 \pm 0.009 \pm 0.046$

## 4 SUMMARY

In conclusion, the total cross section of the reaction  $pp \rightarrow ppK^+K^-$  has been determined for  $p_{beam} = 3.67 \text{ GeV}/c$ . This is the first cross section measurement of the  $pp \rightarrow ppK^+K^-$  channel near threshold, and is equivalent to the inclusive cross section at this beam momentum. The cross section determined here is more than a factor 20 lower than the measured [12] and calculated [15]  $pp \rightarrow K^+ + X$  cross section at the same CM energy above threshold. This large difference in the  $K^+$  and  $K^-$  meson production cross sections in proton-proton collisions is in strong contrast to the nearly equal cross sections measured in sub-threshold heavy ion collisions at the same distance from the respective thresholds. Since this discrepancy between heavy ion collisions and proton-proton reactions has been interpreted as possible evidence for in-medium modifications of the  $K^-$ -nucleon interaction, it would be very useful to study the evolution of the relative  $K^+$  and  $K^-$  meson yields at equal energies from the threshold versus increasing mass number of the colliding nuclei.

### ACKNOWLEDGMENTS

This work has been supported in part by the following agencies: CNRS-IN2P3, CEA-DSM, NSF, INFN, KBN (2 P03B 117 10 and 2 P03B 115 15) and GSI.

### References

- [1] R. Barth et al., Phys. Rev. Lett. 78 (1997) 4007; F. Laue et al., Phys. Rev. Lett. 82 (1999) 1640
- [2] CERN HERA Report 84-01; S. Efremov and E. Paruev, Phys. of At. Nucl. 57 (1994) 532; S. V. Efremov and E. Y. Paruev, Z. Phys. A348 (1994) 217.
- [3] W. Cassing et al., Nucl. Phys. A614 (1997) 415.
- [4] D. Kaplan and A. Nelson, Phys. Lett. B 175 (1986) 57; G. E. Brown et al., Nucl. Phys. A 567 (1994) 937; T. Waas et al., Phys. Lett. B 379 (1996) 34; J. Schaffner-Bielich et al., Nucl. Phys. A 625 (1997) 325; M. Lutz, Phys. Lett. B 426 (1998) 12.
- [5] P. Moskal, Proceedings of the Meson'98 conference, Acta Physica Polonica B 29 (1998) 3091.
- [6] G. Q. Li et al., Phys. Lett. B 329 (1994) 149.
- [7] F. Balestra et al, Nucl. Instr. Meth. A426 (1999) 385.



- [8] H. Calán et al., Phys. Lett. B 366 (1996) 39; A. M. Bergdolt et al., Phys. Rev. D48 (1993) R2969; E. Chiavassa et al., Phys. Lett. B322 (1994) 270; E. Pickup et al, Phys. Rev. Lett. 8 (1962) 329; L. Bodini et al., Nuovo Cimento 58A (1968) 475; A. P. Colleraine and U. Nauenberg, Phys. Rev. 161 (1967) 1387; G. Alexander et al., Phys. Rev. 154 (1967) 1284; C. Caso et al., Nuovo Cimento 55A (1968) 66; E. Colton and E. Gellert, Phys. Rev. D1 (1970) 1979; G. Yekutieli et al., Nucl. Phys. B18 (1970) 301; S. P. Almeida et al., Phys. Rev. 174 (1968) 1638.
- [9] E. Pickup et al, Phys. Rev. Lett. 8 (1962) 329.
- [10] C. Amsler et al., Phys. Lett. B 346 (1995) 203.
- [11] A. Sibirtsev et al., Z. Phys. A358 (1997) 101.
- [12] J. T. Balewski et al, Phys. Lett. B 388 (1996) 859; *ibid*, Phys. Lett. B 420 (1998) 211; R. Bilger et al., Phys. Lett. B 420 (1998) 217; R. I. Louttit et al., Phys. Rev. 123 (1961) 1465; W. Fickinger et al., Phys. Rev. 125 (1962) 2082; G. Alexander et al., Phys. Rev. 154 (1967) 1284; D. Dekkers et al., Phys. Rev. 137; Landolt–Börnstein, New Series I/12b.
- [13] F. Balestra et al., Phys. Rev. Lett. **81** (1998) 4572.
- [14] C. Caso et al., European Physical Journal C1 (1998) 1.
- [15] A. Sibirtsev et al., Z.Phys. A351 (1995) 333.

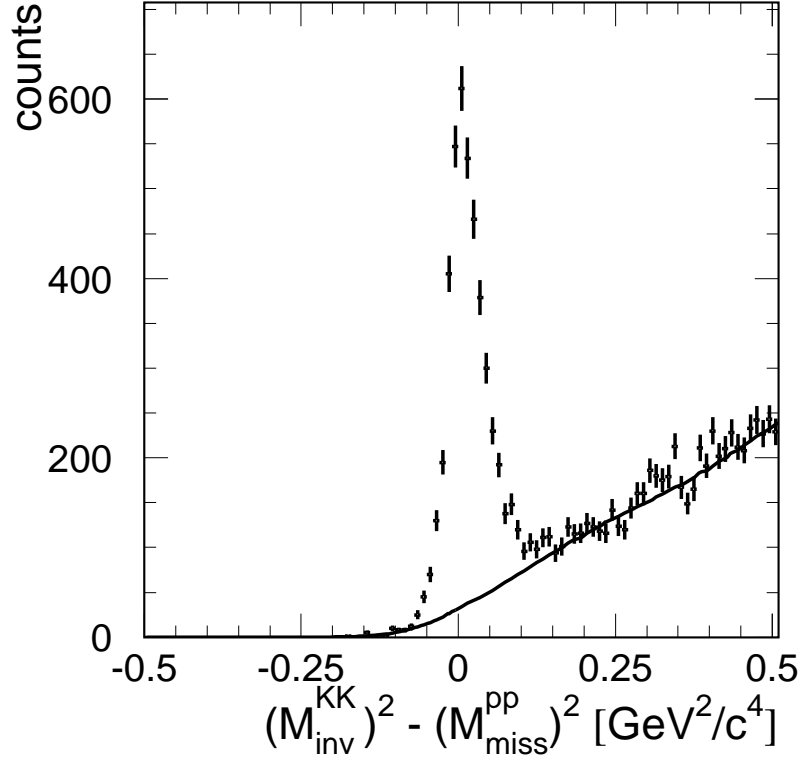


Fig. 1. Distribution of  $(M_{inv}^{KK})^2 - (M_{miss}^{pp})^2$ . The data points are for events with kaon identification and the solid histogram is the scaled background deduced from events without kaon identification.

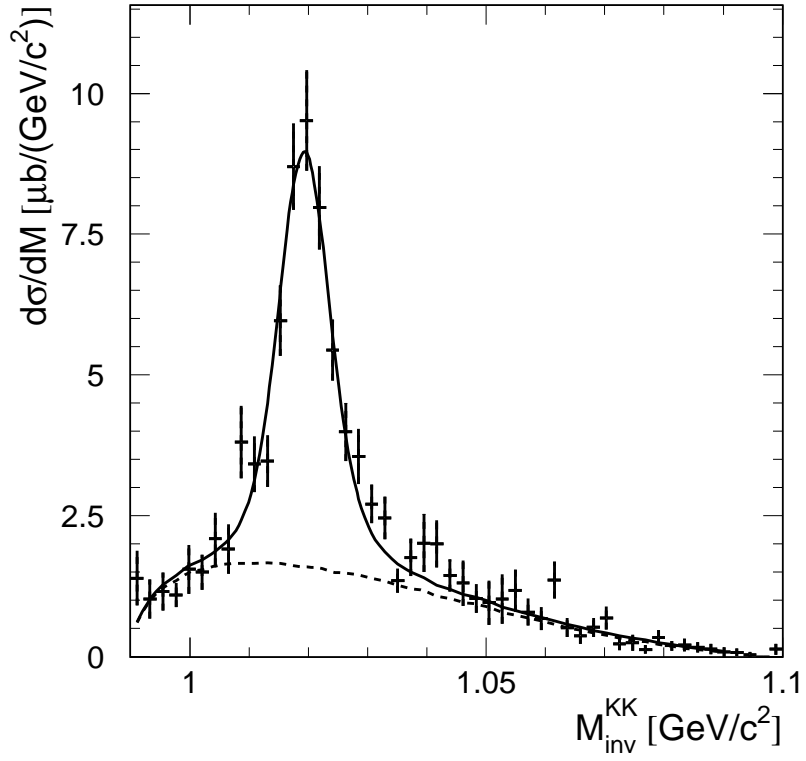


Fig. 2. Spectrum of  $M_{inv}^{KK}$  after acceptance correction and background subtraction. The solid curve is a fit to the data with the sum of a non-resonant  $K^+K^-$  contribution (dashed curve) and the natural line-shape of the  $\phi$  resonance folded with the detector resolution.

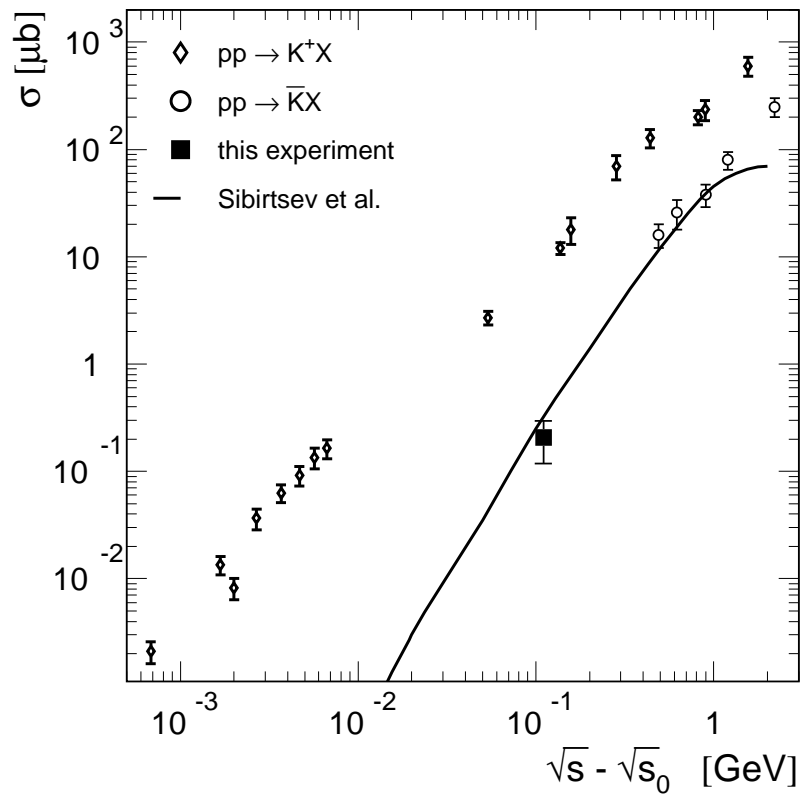


Fig. 3. Total kaon and antikaon production cross sections as a function of the available energy above the appropriate threshold. The present measurement is the solid data point and the open circles are antikaon points deduced from the literature. The curve is a model prediction described in the text and the open diamond points are cross section values for positive kaon production.